An operational flood warning system for poorly gauged basins. Demonstration in the Guadalhorce basin (Spain).

Pierre-Antoine Versini, Marc Berenguer, Carles Corral, Daniel Sempere-Torres

An operational flood warning system for poorly gauged basins. Demonstration in the Guadalhorce basin (Spain)

P.-A. Versini[1,2], M. Berenguer[1], C. Corral[1], D. Sempere-Torres[1]

[1] Centre de Recerca Aplicada en Hidrometeorologia, Barcelona, Spain

[2] Laboratoire Eau Environnemnent et Systèmes Urbains, Ecole Nationale des Ponts et Chaussées, France

Correspondence to: P.-A. Versini (pierre-antoine.versini@leesu.enpc.fr)

Abstract

This paper deals with the presentation of a flood warning system (GFWS) developed for the specific characteristics of the Guadalhorce basin (3200 km^2, SE of Spain), which is poorly gauged and often affected by flash and plain floods Its complementarity with the European Flood Alert System (EFAS) has also been studied. At a lower resolution, EFAS is able to provide a flood forecast several days in advance.

The GFWS is adapted to the use of distributed rainfall maps (such as radar rainfall estimates) and discharge forecasts are computed using a distributed rainfall-runoff model. Due to the lack of flow measurements, the model parameters calibrated on a small watershed have been transferred in most of the basin area. The system is oriented to provide distributed warnings and fulfils the requirements of ungauged basins.

This work reports on the performance of the system on two recent rainfall events which caused several inundations. These results show how the GFWS performed well and was able to forecast the location and timing of flooding. It demonstrates that despite its limitations, a simple rainfall-runoff model and a relatively simple calibration could be useful for event risk management. Moreover, with low resolution and long anticipation, EFAS appears as a good complement tool to improve flood forecasting and compensate for the short lead times of the GFWS.

1. Introduction

Floods represent the most serious natural hazard in Europe, and flood management is a critical component of public safety (Hajat *et al.* 2003; Barredo, 2007). During the last 50 years significant efforts to improve flood warning systems (FWS) have been carried out by the scientific, technical and administration sectors. Thus in the context of medium to large river basins, with response times of the order of tens of hours, forecasts, warnings and public preparedness for reducing casualties from extreme plain floods have clearly improved (Meon 2006). However, the achievements for forecasting flash floods, characterized by short-lasting storms affecting reduced areas of a watershed, have been less impressive. As flood forecasting is in many countries limited to the main streams or to specific watersheds with particular assets like hydropower dams, which are in most cases well-gauged river sections, it leaves large parts of the territory not covered by flood monitoring networks (see for instance: Borga *et al.* 2007; Costa and Jarett 2008; Gaume *et al.* 2009).

A major concern in the context of FWS operating in basins prone to flash floods is to monitor the variability of rainfall in space and time. In particular, the use of radar-based quantitative precipitation estimates (QPE) and nowcasts has been demonstrated to be an interesting tool for anticipating and quantifying the consequences of rainfall at the ground. Radar products are particularly interesting in areas frequently affected by severe storms with complex spatio-temporal patterns (of tens of km^2) and response times of the order of tens of minutes to few hours (see for instance: Sempere-Torres *et al*. 1999; Berenguer *et al*. 2005; Berne *et al*. 2005; Borga *et al*. 2006; Germann *et al*. 2009).

The use of distributed rainfall-runoff models represents a second key element in the production of distributed flow forecasts. Distributed models in general do not seem to perform significantly better than classic simple lumped models when they are used to forecast the discharges at a few specific points of gauged watersheds, although this topic is still a matter of discussion (e.g. Carpenter and Georgakakos 2006; Reed *et al*. 2004). However they provide much richer information than lumped models as they are able to consider the spatial distribution of model inputs (in particular, rainfall) and/or parameters, and produce distributed runoff simulations. In the case of ungauged watersheds,

64 regionalization techniques (see for example Blöschl and Sivapalan 1995) are frequently
65 used to extrapolate model parameters estimated from closest gauged catchment.

66 In this context, two types of warnings can be delivered in the framework of FWS: (i)
67 warnings based on rainfall measurements, and (ii) warnings based on simulated discharges.
68 Both have advantages and limitations.

69 Basically, warnings based on rainfall can be delivered by comparing precipitation
70 accumulations (on different time) to a corresponding reference associated to a probability
71 of occurrence and a return period. As soil moisture condition is not taken into account, the
72 results can sometimes be very different to those based on hydrological simulations (see
73 Alfieri *et al*. 2011). A another well-known approach to issuing warnings based on rainfall is
74 the Flash Flood Guidance, FFG (Georgakakos 2006). The FFG computes the amount of
75 rainfall of a given duration required to cause flooding in a certain basin. If the
76 corresponding observed or forecasted rainfall amounts (integrated for the same duration
77 within the basin) exceeds the pre-computed threshold, a flood warning is issued. The FFG
78 represents a first attempt to evaluate the potential flooding and can be employed at different
79 time and scale resolutions (Norbiato *et al*. 2008). It requires information on the antecedent
80 soil moisture conditions, but does not explicitly compute the discharge responsible for
81 flooding.

82 Alternatively, FWSs may use rainfall-runoff model to issue warnings based on explicit
83 discharge simulations and forecasts. They run at different resolutions depending on the
84 characteristics of the floods that are to be forecasted. Covering whole Europe with a spatial
85 resolution of 5 km, the European Flood Alert System (EFAS, Thielen *et al*. 2009) aims at
86 alerting for floods in trans-national European river basins up to 10 days in advance using
87 model inputs generated with an ensemble weather prediction system. At regional scale,
88 there are several operational FWSs based on discharge simulations. Some examples can be
89 cited: AIGA run by Meteo France[1] in the south-east of France (Lavabre and Gregoris
90 2006), EHIMI run by ACA[2] in Catalonia (Corral *et al*. 2009) and PREVAH, run by WSL[3]

1 French Meteorological Agency

2 Catalan Water Agency

91 in Switzerland (Viviroli *et al*. 2009). Further work is still under development and not yet
92 operational (Reed *et al*. 2007; Javelle *et al*. 2010 for example). Note these regional models
93 can be aggregated at the national scale as the UK National Flood Forecasting System
94 (NFFS) or VIGICRUES run by SCHAPI[4] in France (Tanguy *et al*. 2005). Although they
95 are devoted to a limited area, these regional systems are run at higher resolutions and,
96 consequently, they are more adapted to forecast flash floods. These FWSs are generally
97 based on a similar scheme: the distributed rainfall-runoff model is run to simulate the
98 discharges in several locations of the basin, and these are compared to a database of pre-
99 established flow thresholds to quantify the hazard at each location. A warning is issued
100 when the simulated discharges exceed certain thresholds. The advantage of this method is
101 the use of a discharge value to assess flood hazard. The main weakness generally related to
102 discharge simulation is that model calibration requires stream gauges distributed over the
103 watershed and available historical time series for its calibration.

104 Based on these considerations, a real-time FWS was implemented in 2009 in the
105 Guadalhorce basin (Andalusia, Spain) in collaboration with regional stakeholders interested
106 in flood warning. The main objective was to operationally deliver spatially-distributed early
107 flood warnings, as a tool to raise the awareness of rescue services and increase their
108 preparedness. To suit the short response time and high space resolution required for
109 operational management of this basin, a specific and local FWS (referred to as GFWS
110 hereafter) has been developed. The main challenge the GFWS had to face was the scarcity
111 of stream gauges and the lack of historical hydrometeorological data. In part to overcome
112 this situation, we chose to explore the two approaches presented above: flood warnings in
113 the implemented system are based on both (i) distributed rainfall measurements, and (ii) the
114 discharge simulations obtained with a distributed rain-runoff model.

115 This paper describes the GFWS implemented in the Guadalhorce basin and the
116 methodology chosen to workaround the lack of data. Results obtained during two recent
117 flood events that affected the basin have been analysed. Flood warnings issued with the

---

3 Swiss Federal Research Institute

4 French Hydro-meteorological Nacional Center in charge of Flood Forecasting

GFWS have been compared to effective flooding records collected by the emergency services. In addition, the complementarity between EFAS' low-resolution and long-anticipation warnings and high-resolution and short-anticipation warnings of the GFWS has been analysed from an operational point of view. The lead-times provided by both systems, and the time separating the warning issuance and the inundation occurrence, have been particularly discussed.

The paper is organized as follows. Section 2 presents the framework of study: the Guadalhorce basin and the compilation of historical and real-time hydro-meteorological data. Section 3 describes the distributed hydrological model and the calibration procedure. Section 4 presents the two configurations of the GFWS (based on rainfall and discharge). Two rainfall events that occurred at the beginning of 2010 and caused significant floods are presented in Section 5 as case studies. Section 6 briefly presents EFAS warning system and analyses the warnings delivered for both events. Finally, Section 7 summarizes the main results and concludes on future improvements.

2. Case study:

2.1. The Guadalhorce basin

The Guadalhorce basin (3200 km^2) is located in Andalusia, South of Spain. The river passes through the city of Málaga (500,000 inhabitants) near the outlet of the Mediterranean Sea. The basin is bordered on the West by moderately high mountains (1900 m amsl) and by a low plateau (500 m amsl) on the North. The dominant climate is warm-temperate Mediterranean, characterized by a marked dry season, with hot summers and generally mild winters. The warmest months are July and August with an average temperature of 23ºC, and the coldest season covers the period between December and February with an average of 13ºC. Annual precipitation is comprised between 500 and 600 mm. Rainfall is concentrated during the period October to April (90% of the total amount). Historically, the Guadalhorce river represents a major risk for the city of Málaga and periodically causes floods along its course. Although the region is mainly rural with dominant bare land cover, stakes are numerous, with the population concentrated close to

147 Málaga and many activities related to tourism. For this reason, the regional government of
148 Andalusia has decided to implement an operational FWS with the aim of minimizing risk to
149 people and economic activity.

150 2.2. Hydrometeorological data

151 The studied watershed is covered by a quite scarce measuring instrumentation network. A
152 total of 25 automatic hourly rain gauges are located within or near the basin (see Fig. 1),
153 representing an average density of about one rain gauge per 180 km^2. Such a density can
154 appear insufficient to enable accurate high resolution rainfall estimates through spatial
155 interpolations on small watersheds. Here, time and space scales suited to flash flood
156 dynamics are small: sub-hourly time step and kilometric scale (e.g. Collier 2007; Creutin
157 and Borga 2003; Moulin *et al*. 2009). Nevertheless, this rain gauge network should be
158 enough for larger basins characterized by a response time at least higher than the rain gauge
159 time step. The region of Málaga is also covered by a C-Band Doppler radar operated by the
160 Meteorological Spanish Agency (AEMET). The radar is located at 1173 m amsl and fully
161 covers the basin. The GFWS has been developed to operationally consider radar products
162 characterized by a higher spatio-temporal resolution (1 km^2 and 10 minutes).

163 Four reservoirs and three hourly automatic gauge stations are also located in the upstream
164 part of the Guadalhorce basin: Bobadilla (761 km^2), Ardales (211 km^2), and Teba (202
165 km^2) as illustrated in Fig. 1. They cover a third of the total basin area, leaving the remaining
166 area ungauged (where Málaga is located). Measured discharges are also available in real
167 time for operational purpose. Available historical discharge data have been compiled since
168 2008 to calibrate the rainfall-runoff model.

169 Statistical climate data on historical precipitation are also available (MOPU 1990) as maps
170 of maximum daily rainfall amounts (MOPU 1999), and Intensity-Duration-Frequency
171 curves (IDF), as well as regionalised parameters for the application of the rational Method
172 are described in MOPU (1990).

3. Rainfall-runoff model

A grid-based distributed rainfall-runoff model has been implemented and adjusted with the aim of computing warnings based on simulated discharges at every pixel of the grid inside the area of study. Such a distributed structure allows to take into account the spatial variability of precipitation. Due to the lack of historical hydrological data, and in order to simplify the calibration procedure, the model was chosen to be simple, robust, and depending on a reduced number of adjustable parameters.

3.1. Presentation of the distributed rainfall-runoff model

The Guadalhorce basin has been split into hydrological cells of 1 km^2 that are connected to the outlet of the basin following a simplified drainage network based on the analysis of the topography. To take into account the effect of the three dams, it was considered that the drained area located upstream of each dam does not contribute to cells located downstream. Each 1-km^2 cell is treated as a hydrological unit, where a lumped model is applied. The lumped model employed here is based on the common Soil Conservation Service (SCS) Curve Number (*CN*) method (Mockus 1957) for computing excess rainfall, combined with the linear diffusive wave unit hydrograph for flow routing (Szymkiewicz 2002).

The SCS-CN method assumes that flood flows are essentially composed of surface runoff water or at least fast responding runoff processes. Because of its simplicity and minimal data requirements, the SCS–CN method is widely used in flash flood simulation (see for examples Borga *et al*. 2007; Rozalis *et al*. 2010; Versini *et al*. 2010, 2013). It is based on the water balance equation and a proportionality stating that the ratio of the amount of cumulative infiltration (*F[i]*, in mm) to the amount of potential maximum retention capacity (*S*, in mm) is equal to the ratio of the amount of total runoff volume (*V[i]*, in mm) to the maximum potential runoff volume. The latter being represented by the total rainfall amount from the beginning of the event $P_{tot}[i]$, to which the initial abstraction I_a (both in mm) is subtracted. Assuming $F[i]=P_{tot}[i] - I_a - V[i]$, the total runoff volume generated at the cell scale is computed as:

$$V[i] = \frac{\left(P_{tot}[i] - I_a\right)^2}{P_{tot}[i] - I_a + S} \qquad (1)$$

From this formula, the instantaneous runoff coefficient for time step *i*, $C[i]$, can be deduced. This coefficient has then to be multiplied by the rainfall intensity $P[i]$ to estimate the direct runoff, $Q_f[i]$:

$$C[i] = \frac{\partial V[i]}{\partial P_{tot}[i]} = 1 - \frac{S^2}{\left(P_{tot}[i] - I_a + S\right)^2} \quad (2)$$

Retention capacity *S* is related to the *CN* coefficient which is usually estimated from the soil properties and taking a value between 0 and 100. The original SCS equation was adjusted for events with large amounts of precipitation accumulated during long periods (several days). Thus, when the total amount of precipitation increases during an event, the soil drainage process is not explicitly represented and there is no possibility for the system to recover the basin's water retention capacity. The instantaneous runoff coefficient increases simultaneously and the simulated direct runoff has a strong tendency to be overestimated. In this study, an attempt was made to take into account the process accumulating rainfall on an adapted time period. After several tests, a period of 24 hours has been arbitrarily chosen to accumulate rainfall:

$$Q_f[i] = P[i] \cdot \left[1 - \frac{S^2}{\left(P_{24h}[i] + S\right)^2}\right] \quad \text{when } P_{tot}[i] > I_a \quad (3)$$

$$Q_f[i] = 0 \quad \text{otherwise}$$

Where $P_{24h}[i]$ is the amount of precipitation in a 24-moving window which ends at time step *i*, and from which the initial abstraction *Ia* is deduced.

Additionally, the conceptual function proposed by Weeks and Boughton (1987) has been chosen to model the slow flow $Q_s[i]$:

$$Q_s[i] = \Delta t \cdot \alpha \cdot Q_f[i] + Q_s[i-1] \quad \text{if} \quad Q_f[i] > 0 \quad (4)$$

$$Q_s[i] = Q_{ini} + \left[Q_s[i-1] - Q_{ini}\right] \cdot \left(1 - \Delta t \cdot \alpha\right) \quad \text{if} \quad Q_f[i] = 0 \quad (5)$$

223 Where α (with units of time^{-1}) is a parameter to calibrate, Δt is the time step, and Q_{ini} is the
224 initial flow computed with the observed runoff at the beginning of the event.

225 It assumes that there is a constant ratio between the runoff component $Q_f[i]$ and the
226 variation of the slow component between two time steps. Base flow is also recursively
227 estimated from the previous value. It is initialized with the initial flow Q_{ini} measured in
228 gauged cells at the beginning of the event, and extrapolated to the rest of the basin
229 proportionally to the drainage area of each cell. When there is no direct runoff, the
230 recession curve $Q_s[i]$ becomes exponential. We have verified that the base flow assumption
231 made does not affect the mass balance, and it is beneficial to improve the representation of
232 the simulated discharge.

233 The total runoff $Q_{tot}[i]=Q_f[i]+Q_s[i]$ generated at each cell is then routed downstream
234 following the drainage network. A single unit hydrograph based on the linear diffusive
235 wave function and Muskingum parameters (Szymkiewicz 2002) has been used:

236 $$HU[i] = \frac{1}{\sqrt{2\pi \cdot (1-2X)}} \cdot \frac{N}{K} \cdot \left(\frac{K}{i \cdot \Delta t} \right)^{\frac{5}{2}} \cdot \exp\left[- \frac{(i \cdot \Delta t - N \cdot K)^2}{2 \cdot (1-2X) \cdot K \cdot i \cdot \Delta t} \right] \quad (6)$$

237 Where $HU[i]$ is the unit hydrograph at time step i, X is the weighting factor (dispersion
238 parameter) that varies between 0 and 0.5, K is the storage time for one path, and N the
239 number of paths of the course.

240 A specific unit hydrograph (HU) is defined for both kind of cell. One first HU is applied in
241 each cell to represent the hillslope flow propagation. Then a second is applied on the river
242 course connecting the hillslope cell to the downstream point of interest to represent the
243 propagation of the stream flow. The linear diffusive wave function can represent both
244 processes changing its parameters. For each cell, both hillslope and river routing parameters
245 (N, X, K) need also to be adjusted.

246

3.2. Reduction of the number of parameters to calibrate

As described above, the number of parameters to adjust is rather large. It has to be reduced to make the model robust and to limit uncertainty due to over-parameterisation (see Perrin *et al*., 2001): (i) spatially distributed *CN* [used in Eq. (3)], the base flow parameter α [see Eq. (4) and (5)] for the loss function and, (ii) spatially distributed routing parameters for both hillslope (N_h, X_h, K_h) and river (N_r, X_r, K_r) routing functions.

An *a priori* method has been used to estimate distributed *CN* values over the entire watershed. Geomorphological data (slope, geology and land cover) at cell scale have been used to compute the *CN* distribution within the basin with a 1-km resolution according to the recommendations of the Spanish Ministry of Public Works (MOPU 1990). Previous studies based on this method (Corral *et al*. 2000; 2002) have shown significant differences between effective field capacities and those obtained with this *a priori* method: simulated discharges have a clear tendency to be overestimated. For this reason, an average curve number correction factor (*FCN*) has been calibrated to scale the map of *CN* values. Note that this kind of correction was already used in Borga *et al.* (2007) for example.

In many applications of the SCS method, the initial abstraction I_a does not take into account antecedent moisture condition and is deduced from the potential maximum retention *S*. In this study, I_a is not considered as a parameter and is assumed to be independent of *S*. It is firstly approximated as the difference between the total amounts of antecedent evapotranspiration and rainfall over the previous 15 days. Then, I_a is updated in real time from stream gauge measurements identifying by means of the hydrograph initial rising time (see more details in Corral *et al.* 2002). I_a represents the total amount of precipitation from the beginning of the event to the first initial hydrograph rising time (deducing the response time of the watershed).

The three parameters that govern both hillslope and river routing functions have also been simplified. Concerning the hillslope function, N_h is fixed to one path, and X_h to 0 representing a maximum attenuation in peak discharge. Concerning the river function, applied on the river course to the outlet, N_r is assumed to represent the number of cells until the outlet; the remaining weighting factor X_r needs to be calibrated and is assumed to be

uniform over the basin. Both storage times K_h and K_r are computed as the ratio between hillslope or river course lengths (derived from the DTM) and flow velocities. These velocities v_l and v_r are also considered uniform over the basin and represent the last parameters to be calibrated.

Summarizing, the adjustment of the model required the calibration of 5 parameters: the curve number correction factor (FCN), the base flow parameter (α), and three routing parameters [hillslope velocity (v_h), river velocity (v_r), river weighting factor (X_r)].

3.3. Adjustment of the parameters

The rainfall-runoff model described above has been calibrated using observed discharges available at the gauged watersheds (see Section 2). Eight rainfall events for 2008 have been selected for the adjustment of the model parameters. Radar data were not available for this period, so spatially interpolated rain gauge data have been used. The total rainfall amounts of these events were not very large (between 20 and 100 mm). The calibration of the model has been carried out with the observations measured at the Bobadilla stream gauge (no significant discharges were measured at the two other stations and/or the data were not available). Because the number of interesting rainfall events was rather small, we chose to calibrate the model manually, and to reproduce the most intense events. The results have been evaluated with the Nash criterion (Nash and Sutcliffe 1970) and are summarized in Table 1.

The performance of the model in term of Nash efficiency varies from one rainfall event to another. The simulations accuracy is acceptable in the light of the results obtained in comparable case studies (ungauged basins or poor instrumented framework), for which the model calibration was made with a longer historical database (for example: Borga 2008; Versini *et al*. 2010). The performance of the model is generally better for the largest rainfall events, where the effort of calibration was made (the more significant events are represented on Fig. 2). The hydrological response to smallest events appears a little more erratic and is probably linked to the non-linearity of the rainfall—runoff transformation. In this case, initial abstraction plays a major role and can strongly affect the simulated

discharges. Note that to achieve reasonable simulations, a curve number correction factor FCN of 0.5 has been chosen, implying that the map of CN calculated a priori, strongly overestimate discharges. This value may seem rather large, but tends to be common in flood simulation in Mediterranean basins (see Corral *et al*. 2002; Francés and Benito 1995).

Rainfall estimates based on spatial interpolation of rain gauge measurements could also represent a source of uncertainty. The coverage of the current rain gauge network may be insufficient to estimate reliable distributed rainfall in the gauged watershed used for calibration (Bobadilla), where no rain gauge is available inside (see Fig. 1). This may partially explain the differences between simulated and observed discharges.

The calibration of the rainfall-runoff model has been carried out under a number of limitations (given the scarcity of data, number of rain gauges, model structure…) that may have a significant impact on the performance of the model. This needs to be considered when analysing the results of the GFWS. Post-flood field investigation and new time series, as they become available, may be used to improve the rainfall-runoff model (specially its calibration).

Finally, the values of the parameters calibrated in the Bobadilla stream gauge (i.e. FCN, α, v_h, v_r and X_r-) have been transferred to the remaining (ungauged) part of the basin, implicitly assuming a similar hydrological behaviour.

4. The GFWS

The purpose of the GFWS, presented here, is to provide distributed warnings based on rainfall accumulations and runoff simulations (at the same resolution of 1 km^2). In the current configuration, the warnings are computed at each time step from all the precipitation data available up to the present. Three different types of warnings related to hazard probability expressed in terms of return periods are delivered. Two of these are based on rainfall estimates and one on simulated discharges. Note that because of data collection and fast response of small basins, lead times provided by the GFWS are quite short (usually of the order of 1 hour).

4.1. Warnings based on rainfall estimates

Without taking into account any hydrological process, the distributed rainfall data can bring a first interesting attempt related to the expected consequences of the rainfall event and to localize the potential inundations. Two different types of warnings can be computed for every cell of the studied area and using these precipitation fields: (i) based on estimated rainfall at point locations (cells of 1 km^2), (ii) based on spatially aggregated rainfall at each point (i.e. accumulated within the area upstream of each point). These warnings have the advantage to be computed quickly and effectively, without any information other than rainfall.

4.1.1. Use of IDF curves

IDF curves are used as a benchmark for estimating the return period associated with a given rainfall. IDF curves are widely used, and different techniques exist to compute them [see Ben-Zvi, (2009) for an exhaustive review]. In Spain a common methodology is that recommended by the Spanish Ministry of Public Works for drainage design studies (MOPU 1990). It has been chosen in this study and has the following synthetic expression:

$$P_D(T) = \frac{P_{24h}(T)}{24} \cdot FR^{\frac{28^{0.1} - D^{0.1}}{28^{0.1} - 1}} \quad (7)$$

Where $P_D(T)$ is the rainfall (in mm) associated with a duration D (hours) and a return period T, $P_{24h}(T)$ is the daily accumulated rainfall (mm) for a return period T, and FR is a regional factor equal to 8.5 for the area of study.

The extension of IDF to radar rainfall estimates is not straightforward (as illustrated in Norbiato *et al.* 2007 and Wright *et al.* 2013). IDF curves are usually developed from rain gauge networks that are often characterized by low spatial density and short observation periods. Moreover, point-to-area transformation is achieved through area reduction factors ignoring local rainfall climatology or storm type (see section 4.1.3). Despite these limitations, the Spanish methodology has been applied here. Finally, IDF maps have been calculated with a resolution of 1 km2, for different return periods (2, 5, 10, 25, 50, 100, 200 and 500 years) and different durations (1, 2, 3, 4, 6, 12 and 24 hours) for both point and spatial aggregated rainfall.

4.1.2. Warning based on point rainfall

This type of warning is calculated from the point rainfall measurements accumulated during one hour. It is assumed that this accumulation time is relevant to deliver information about the most critical situations at cell scale. It could be of interest for issuing warning in urban environment or for very sensitive points such as roads (e.g. Versini *et al*. 2010). The warning computation is based on a direct comparison, cell to cell, between estimated rainfall, and the IDF threshold values computed for D=1 hour and different return periods T. The value assigned to the warning in a particular cell is the maximum of the return period values that has been exceeded by accumulated rainfall estimates.

4.1.3. Warnings based on aggregated rainfall

In this case, the warning is computed to represent as well as possible the consequences of rainfall at watershed scale (every cell draining an area larger than 4 km^2). With this aim, rainfall is accumulated for a duration D equal to the estimated concentration time of the basin. This concentration time is obtained from both river length and average slope data according to MOPU 1990). These same recommendations propose a correction factor to diminish the thresholds for areal rainfall amount which depends on the drained area S:

$$k = 1 - \log\left(\frac{S}{15}\right) \qquad \text{when } S > 15 \text{ km}^2 \tag{8}$$

$$k = 1 \qquad \text{otherwise}$$

4.2. Warnings based on simulated discharges

Warnings based on simulated discharges are computed with the distributed rainfall-runoff model for every cell where the drained area exceeds 10 km^2. At these locations, the simulated discharges are compared with peak flow thresholds estimated for return periods T={2, 5, 10, 25, 50, 100, 200, 500 years}. They are based on the Rational Method, as described in MOPU (1990).

5. Test case studies

The GFWS started operating in May 2009. Little after, two serious rainfall events occurred (in January and February 2010), both resulting in significant flooding in the region of Málaga. These two events were not used in the calibration of the rainfall-runoff model (see Section 3.3), and resulted the largest accumulations since the GFWS has started. As weather radar observations were not available for these events, the rainfall field was estimated by spatial interpolation of rain gauge measurements with a resolution of 1 hour. A third event has been selected. It corresponds to a minor event for which the C-band radar of the Spanish Meteorological Agency (AEMET) located near Málaga was operating. Although no inundation occurred during this event, it illustrates the use of radar QPE. The events and the associated performance of the GFWS are presented herein, also considering the information on the inundations in the Guadalhorce basin reported by the emergency services.

5.1. Event of 6-7 January 2010

5.1.1. Description of the rainfall event

The maximum observed accumulations reached up to 70 mm on the southern portion of the Guadalhorce basin (see Fig. 3-a). The event started at about 23:00 UTC on 6 January 2010 and lasted for 12 hours. However, most of the precipitation was registered between 08:00 and 10:00 UTC (during this period rain gauges around Málaga registered accumulations of 40 mm) as a consequence of a mesoscale convective system sweeping the basin.

The intense precipitation registered in the morning of 7 January caused flooding of houses, basements, garages and streets, mainly in the suburbs of Málaga and in Alhaurín de la Torre (Fig. 4): emergency services registered a hundred flooding incidences between 9:00 and 10:00 UTC in these two cities. These areas are frequently affected by inundations and this event illustrates a typical case of urban flash flood due to an intense storm that is not rare in southern Andalusia.

During this event, two of the three stream gauges of the basin (Bobadilla, Teba) operated normally. These gauges (see Fig. 1) are located far upstream from the area mostly affected by precipitation (around the city of Málaga), and the total precipitation amounts in the sub-catchments drained at these points were relatively minor (around 30 mm). Consequently, the resulting observed discharges were not significant (see Table 2).

5.1.2. Performance of the GFWS

The comparison between stream gauge observations and the simulations obtained with the rainfall-runoff model at these locations show some agreement, as quantified in terms of the Nash efficiency (presented in Table 2). It is worth noting the performance of the model at the stream gauge in Teba, whose measurements were not used in the calibration of the rainfall-runoff model (stated in Section 3.3).

The GFWS was able to issue warnings in the areas where flooding actually occurred. Fig. 4 shows the maximum warnings based on point rainfall (issued at 9:00 UTC), and based on aggregated rainfall and simulated discharges (both at 10:00 UTC). Concerning the former (Fig. 4a), a warning was issued around the city of Málaga and matching the area where the most intense convective cell affected the basin. The core of the warning (in green) corresponded to an hourly intensity over 35 mm/h, which correspond to a return period of around 5 years. Around this core, the 2-year return period warning level was reached in the blue area (which corresponds to an average hourly intensity over 25 mm/h). These patterns had some correspondence with the flooding that occurred in this area between 9:00 and 10:00 UTC. These warnings were confirmed by those based on aggregated rainfall and simulated discharge in the area. Because these two use information on the spatial structure of the basin, they have advantage to localize more precisely the location of potential flooding. Both predicted the maximum threat of flooding at 10:00 UTC West of Málaga (Fig. 4-b and 4-c), where a small tributary stream crosses the suburbial industrial area, and at Alhaurín de la Torre (respectively, draining basins of 30 and 73 km^2). Both criteria were consistent with each other and only differed on the assigned return periods: 2 years when assessed based on aggregated rainfall and 5 years when the computations are based on simulated discharges. This difference is due to the estimated initial abstractions almost

equal to 0. In any case, these warnings coincided very well with the reaches where flooding was reported within the basin.

5.2. Event of 15-16 February 2010

5.2.1. Description of the rainfall event

There are clear differences between this rainfall event and that presented in Section 5.1: Rainfall intensities were much lighter, maximum hourly intensities hardly exceeded 20 mm/h, but it lasted significantly longer (it did not stop raining for about 24 hours), which resulted in progressive saturation of the soils of the basin. The area located near the coast was particularly affected, with substantial amounts of rainfall registered in Alhaurín de la Torre (totals reached up to 215 mm -nearly a third of the mean annual precipitation), and over 100 mm around Málaga (see Fig. 3-b). In terms of daily rainfall, and according to MOPU (1990), the 50 years return period (180 mm) was exceeded in Alhaurín de la Torre, and it was between 5 and 10 years (90 and 115 mm, respectively) in Málaga. Along the event, the accumulated precipitation caused several floodings in the morning of 16 February 2010 (after 24 hours of precipitation). The rescue services did more than 40 actions related to flooding (essentially homes and garages) in several municipalities in the province of Málaga: Alhaurín de la Torre, Coín, Campanillas and Cártama (see Fig. 5). These actions included the use of helicopters to evacuate people trapped at home or in flooded roads.

As in the previous event, the largest rainfall amounts occurred downstream the gauged watersheds (50 and 20 mm in the sub-basins of Ardales and Bobadilla, respectively). As a result, observed discharges were not significantly high, and the observed peaks were comparable to those of 6-7 January 2010 (see Table 2).

5.2.2. Performance of the GFWS

The hydrographs simulated with the rainfall-runoff model can be considered acceptable in terms of the Nash efficiency (see Table 2). Despite of the rough calibration, the model seems to reproduce correctly the hydrological response at the location of stream gauges.

The GFWS was able to issue consistent warnings in the flooded areas depending on the type of warning used (based on rainfall or simulated discharge). As explained above, the large rainfall accumulations recorded during this event were the result of the long duration of the event, rather than very intense precipitation. As a result, observed precipitation intensities did not exceed the thresholds to issue warnings based on hourly point rainfall at any time: The highest observed intensity in the basin was around 20 mm/h, lighter than the average value for the 2-year return period around 25 mm/h.

The highest warning levels issued based on aggregated rainfall and simulated discharges are presented in Fig. 5 (at 6:00 and 7:00 UTC, respectively). Aggregated rainfall exceeded the 2-year return period for the first time at 03:00 UTC in the main stream between Coín to Málaga. The levels progressively increased and at 6:00 UTC the 5-year return period was exceeded. At the same time, small tributaries to this main stream were also marked as potentially flooded. It is clear how the areas where the warnings were issued match the points where the main floods actually occurred (Alhaurín de la Torre, Coín, Cártama, and Málaga, circled with solid red ellipses), being the only exceptions Campanillas and the suburbs of Málaga where no warning was issued. After 3:00 UTC, warning levels decreased and remained only for the main stream. At 12:00, 4 hours after the rainfall had ceased, only the Guadalhorce stream located between Cártama and Málaga was identified as a risky area and remained so until the end of the day.

Warnings computed from simulated discharges were more intense and more numerous than those already calculated with the aggregated rainfall (the estimated initial abstractions were null). Indeed, the first warning appeared at 23:00 UTC, and at 3:00 UTC exceeded the return period of 5 years (i.e. higher than the 2-year one issued for aggregated rainfall). At 7:00 UTC, the simulated discharges passing through Cártama and Alhaurín de la Torre were exceeding the 25-year return period, and in Coín, Campanillas and Málaga, the 10-year return period. The simulated peak discharge in Málaga outlet occurred at 10:00 and reached a value of 817 m^3/s, although rescue services, based on ground observation, estimated the discharge to temporarily exceeded 2000 m^3/s. The fact that drained area located upstream of each dam were not considered can explain this large difference. Warnings based on simulated flows, thus, corresponded very well with the floods that

500 occurred in this area. Unlike for the warnings based on aggregated rainfall, the flooding in
501 Campanillas and the suburbs of Málaga at 7:00 UTC (see Fig. 5-b) were not missed:
502 warnings of 10- and 5-year return period were issued at these points, respectively.

503 A flood warning (5-year return period) was also issued for the Ardales stream, downstream
504 of one of the dams of the basin (Conde Guadalhorce dam, surrounded in Fig. 5-b), where
505 no problem actually occurred. This area is not anthropized and for this reason was not
506 affected. As the simulated discharge was not propagated downstream the dam, no warning
507 was issued further.

508 ## 5.3. Event of 21 April 2011

509 ### 5.3.1. Rainfall inputs: processing of radar data

510 The very-high resolution of radar QPE products both in space and time (for the case of the
511 Málaga radar, 1km and 10 minutes) fits very well the requirements of flood monitoring in
512 fast response basins such as the Guadalhorce basin, as it allows an accurate representation
513 of the variability of the rainfall field and capture local intensities that could be missed by
514 rain gauge networks. However, radar measurements require a thorough processing to
515 convert them into Quantitative Precipitation Estimates.

516 In our case, we have implemented the chain of algorithms of the EHIMI package (Corral *et*
517 *al*. 2009), which includes: (i) reduction of the effects of beam blockage by the orography
518 using the approach of Delrieu et al. (1995), (ii) clutter elimination with the technique of
519 Sánchez-Diezma et al. (2001), (iii) identification of the type of precipitation and
520 extrapolation of elevated reflectivity measurements to the surface according to a double
521 Vertical Profile of Reflectivity as described by Franco et al. (2006, 2008), and (iv)
522 conversion of reflectivity into rain rate using a double Z-R relationship for stratiform and
523 convective rain. Hourly accumulations were generated from instantaneous rainfall maps
524 with an algorithm similar to that of Fabry et al. (1995).

5.3.2. Description of the rainfall event

The river rise of 21 April 2011 is the result of a widespread system that crossed Andalusia from west to east. Over the basin, 10 mm of rainfall were accumulated in 10 hours (approximately from 14:00 UTC to 24:00 UTC), with totals locally reaching up to 25 mm near Málaga and on the southern portion of the Guadalhorce basin (see Figure 6-a). The most intense precipitation was concentrated at about 17:00 UTC with local hourly intensities around 20 mm/h.

The event accumulation based on radar measurements does not show the artefacts that frequently affect radar rainfall products (due to e.g. sub-estimation "corridors" due to beam blockage or systematic holes from ground clutter filters). It is also noticeable that radar-based QPE values at gauge locations reasonably matches rain gauge records inside the basin (the differences can be attributed to remaining errors in radar QPE, errors in rain gauge measurements and representativeness errors, since the two systems measure rainfall at different scales).

5.3.3. Performance of the GFWS

During 21 April 2011, the GFWS did not deliver any warnings whatever the type (based on point rainfall, spatially aggregated rainfall or simulated flows). Despite some intense precipitation, no significant increase in discharge was noticed and no alert thresholds were exceeded. The propagation of rainfall through the drainage network reduced the magnitude of the hazard, which was already low in terms of point rainfall.

However, the benefit of using radar-based QPE is illustrated by the location of intense precipitation (about 20 mm/h) around Málaga and in the central part of the basin at 17:00 UTC. As shown in Figure 6, there is no rain gauge at the location where the most intense precipitation occurred, and the field interpolated from rain gauges did not reproduce these local rainfall intensities (or any warning, see Fig. 6-c). Despite some possible overestimation of the radar-based QPE, this proves the use of weather radar may provide a better understanding of intense rainfall away from the rain gauge network. These differences could have been even more significant for more convective situations characterized by very intense local rainfall.

554 It has to be noticed that no flooding occurred during this event. This is also a satisfactory
555 result for the GFWS, which can be interpreted as follows: First, spatial distribution of
556 precipitation represented by radar-based QPE indicate the location and timing of the highest
557 intensities, which can identify the possible consequences caused by direct rainfall as it may
558 be the case of local floodings in urban areas. Second, the absence of warning in the river
559 network shows there was no significant consequence in terms of discharges, showing that,
560 for this particular case, the rainfall-runoff model did not overestimate the discharges
561 produced by moderate rainfall.

562 **5.4. General comments**

563 Regarding the two examples for which flooding occurred, warnings based on point rainfall
564 seem to be well adapted to prevent from the consequences on the ground of intense
565 precipitation. They are particularly useful to alert of urban flood where the rainfall is
566 directly responsible for flooding. As the current GFWS does not take into account urban
567 drainage (which requires a cadastral resolution), theses warnings could be sufficient to
568 localize the areas prone to flooding during intense precipitation event.

569 Although the model was calibrated for only one gauged basin and for few rainfall events,
570 the results computed with the rainfall-runoff model for these two recent events are rather
571 satisfactory: the simulated discharges calculated at the other stream gauges locations are
572 quite similar to the observed ones. The fact that only warnings based on simulated
573 discharge have pointed out every effective flooding for both events, illustrates the interest
574 of working with a distributed rainfall-runoff model. This rather positive result could, at
575 least in part, be attributed to the significant magnitude of the events, especially given the
576 limitations of the model calibration.

577 Moreover, return period characterizing warnings based on simulated discharges appear to
578 be higher than those based on aggregated rainfall for both studied rainfall events. Regarding
579 the consequences at the ground and the frequency of the total amount of precipitation
580 locally measured, discharge return periods seem to be the more representative. In these
581 cases, the underestimation of aggregated rainfall-based warning may be due to different
582 reasons. First, this method has intrinsic limitations due to the non-consideration of rainfall-

runoff transformation. Second, the antecedent soil moisture conditions, which have a significant role in the catchment response (see e.g. Merz and Blöschl 2009), is not considered. Despite the basic function used to estimate initial losses, the rainfall-runoff model is able to take into account soil moisture *via* the parameter I_a in Eq. 3. For both studied events, the estimated initial abstractions were almost equal to 0, which result to increase the amount of water producing runoff.

These provisional remarks have to be taken with caution because based on the analysis of only two events. They have to be confirmed in the future by studying the performances of the GFWS for new rainfall events.

6. Combined use of EFAS with the GFWS for flood forecasting

6.1. The European Flood Alert System (EFAS)

The European Flood Alert System (Thielen *et al*. 2009) issues flood warnings based on probabilistic flood forecasts with lead times up to 10 days at European scale. It is based on the hydrological model LISFLOOD (Van Der Knijff *et al*. 2010) and rainfall inputs come from a medium-range ensemble weather predictions (NWP-EPS), consisting of a first set of 51 members generated at the European Centre for Medium-range Weather Forecasts (ECMWF) over a 80-km grid, and a second set of 16-member ensemble from the COSMO Consortium (COSMO-LEPS), run at 10-km grid resolution. Both sets of weather forecasts are included in the hydrological model to produce two ensembles of 51 and 16 members of flow forecasts. The hydrographs generated in such a way are then analysed to issue early warnings on the basis of a threshold exceedance analysis.

LISFLOOD was not adjusted for the Guadalhorce basin using discharge measurements (as it is for other European catchments). However, the discharge thresholds associated to flood warnings are directly defined based on a statistical analysis of simulated discharges over a historical 30-year period. The highest discharge obtained from these long-term simulations is used to set the “severe” situation (that is, when the model outputs exceed the 30-year maximum flow situation, a “severe” warning is issued). Similarly, the discharge value

corresponding to the 99% percentile of historical flow simulations is chosen as the threshold for which a "high" warning is issued. When comparing "high" discharges with records from level gauges in Europe where the model was calibrated, Thielen et al. (2009) reported that the value obtained for "high" warnings usually corresponds to return periods around 1 to 2 years.

6.2. EFAS forecasts for the studied events

EFAS did not issue any warning in advance for the case of 6-7 January 2010 (neither for 21 April 2011), since rainfall accumulations were due to a local and intense rainfall core that NWP-EPS had missed.

Alternatively, for the second event (15-16 February 2010) the NWP-EPS did depict the main space and time features of the rainfall field. Consequently, EFAS delivered flood warnings with an anticipation of four days: probabilistic forecasts issued a significant flood warning on the main stream of the Guadalhorce River between the 3 dams and Málaga, leaving the secondary streams (where most of the inundations occurred) safe. From the 51 ECMWF members, 80% forecasted floods, whereas the simulations of 2 of the 16 COSMO members exceed the threshold of "high" level 4 days in advance (8 out of 16 members 2 days in advance). For this second event, the outlet peak flow simulated with LISFLOOD was around 160 m^3/s. Although this is enough to exceed the "high" level warning in the Guadalhorce basin (around 142 m^3/s, and, as discussed above, corresponding to a 1-2 years return period), it is far from the maximum discharges simulated with the GFWS (817 m^3/s in Málaga) and the 25-year return period obtained for the GFWS simulations (see section 5.2). We believe that the latter may be more accurate as it matches better the reports of local rescue services, which had not faced similar flooding for 20 years (reports based on eye witness estimated the peak flows in about 2000 m^3/s, higher than the 100-year return period). It is worth insisting on that the version of EFAS currently running in the Guadalhorce basin is uncalibrated, and, therefore, flow simulations cannot be interpreted in absolute terms. Also, it is necessary to remark that no intermediate threshold is established between the "high" and "severe" warnings, which in cases such as the one analysed here could have helped. Note that a more general discussion on the matching between simulated discharges and reference thresholds is conducted in the last section.

6.3. Use of EFAS warnings to extend lead-time

In the case studies, most of the watersheds responsible for flooding are small (less than 100 km^2) and, consequently, characterized by short response times (less than 1 hours). In the operational framework, GFWS warnings based on weather radar and/or rain gauges measurements require the collection of rainfall measurements (which, currently, takes up to 20 minutes). This means that it takes very short time after the warnings are issued for the inundations to occur in the smallest watersheds (or even equal to 0). This is often insufficient to prevent the concerned population from the flooding. Recent works (e.g. Creutin *et al*. 2009; Siccardi *et al*. 2005) have shown that when the social response time is longer than the catchment response time, the planning of management measures requires the use of forecast rainfall fields such as NWP-EPSs. That is why mid-term rainfall forecasts and EFAS warnings represent a good complementary tool for the GFWS. Delivering these forecasts some days in advance, despite the rough spatial accuracy, can be useful from a practical point of view. They can be used as pre-alarms to inform decision-makers about a possible flooding and advise the population, for example, to reduce their trips and to protect vulnerable items. Similarly, emergency services can prepare their teams and anticipate their future actions around the areas of possible flooding to intervene more rapidly the day in question. According to this configuration, the warnings issued by EFAS on the main stream of the Guadalhorce for the 15 and 16 February 2010 could help to limit damages. Warnings issued by the GFWS could have then been used to act more precisely on the affected tributaries.

7. Discussion and Conclusion

A local Flood Warning System has been implemented in the Guadalhorce basin, frequently affected by plain floods and flash floods. The system delivers distributed warnings over the entire basin based on the available sources of information: rainfall estimates and runoff simulations are compared to pre-computed values of hazard probability (separately for rainfall and runoff) to determine the warning level expressed in terms of return period.

The performance of the GFWS has been demonstrated on two major events that occurred in the basin at the beginning of 2010 (the most intense since the system is operating). In general, the warnings issued by the system matched the timing and location where actual

671 inundations occurred. The performance of the system during the presented cases has shown
672 how the different warnings (based on rainfall estimates or on flow simulations) are well
673 adapted to the types of hazard that affect the Guadalhorce basin. Indeed, results obtained
674 for 7 January 2010 confirm that warnings based on point rainfall are well adapted to alert of
675 urban or flash floods, as they are driven by very intense precipitation. As urban drainage is
676 not considered in the system, the precise location of intense rainfall could be enough from
677 the end-user point of view. On the other hand, results obtained on 16 February 2010
678 illustrate the effectiveness of warnings based on aggregated rainfall and discharge
679 simulations to forecast the inundations caused by stream overflows.

680 Moreover, on the analysed events, a significant difference has also been noticed between
681 the return period characterizing warnings based on aggregated rainfall and simulated
682 discharges. Those calculated with the rainfall-runoff model, usually higher, have also
683 pointed out every effective flooding. This underlines the importance of taking into account
684 rainfall-runoff transformation and antecedent soil moisture conditions.

685 In parallel, the European Flood Alert System (EFAS) has proved to be a valuable
686 complementary tool for flood warning. It forecasted the consequences of the larger-scale
687 and long-lasting event of 15-16 February 2010 four days in advance. Although it did not
688 forecast the exact location of flooding and underestimated the magnitude of the event, it
689 provided useful information to prepare the emergency services to operate. However, EFAS
690 did not anticipate the event of 7 January 2010, for which GFWS showed a good
691 performance. We attribute this miss mainly to the inability of the NWP-EPS model to
692 depict the intense but very local precipitation system that produced the event. This kind of
693 events show the interest of rapid-updating and high-resolution FWSs to issue warnings at
694 resolutions that are closer to the scales at which flooding occurs in this basin (for the
695 analysed events most of the inundations occurred in secondary streams for which EFAS
696 does not produce flow forecasts).

697 The presented results illustrate the interest of using the GFWS for flood warning in the
698 Guadalhorce basin, but it has to be recalled that this analysis is based on the study of only
699 two rainfall events. These conclusions need to be confirmed in the future regarding the

700 performance of the GFWS on new events. In addition, there are a number of implicit
701 hypotheses and limitations that are worth discussing:

702 (1) The selection of thresholds for issuing warnings with GWFS is arbitrary according to
703 the usual practices in Spain (i.e. according to the MOPU 1990 and 1999 for runoff and
704 rainfall respectively). This is so because long series of observations are inexistent in the
705 basin. In particular, the method used for setting flow warning thresholds uses historical
706 daily rainfall accumulations (implicitly assuming a very simple rainfall-runoff model to
707 estimate design peak flows). This results in some sort of inconsistency when the discharges
708 simulated with the rainfall–runoff model presented in section 3 are compared to the
709 thresholds established with an obviously different model. The availability of longer series
710 of hydrological records would allow establishing better thresholds (e.g. as suggested by
711 IACOW 1982 and Reed *et al*. 2007). In any case, the used thresholds can still be considered
712 as indicators of the relative degree of severity of the events, despite the fact that the
713 associated return periods cannot be taken in absolute sense. For example the results
714 presented above show a clear correspondence between the issued warnings and the reported
715 inundations, and indicate relative significance of the events, but cannot be considered
716 extreme (the 100-years return period was certainly not exceeded).

717 (2) The number of hydrometeorological sensors (both rain and stream gauges) in the basin
718 poses an important challenge for the performance of the GFWS. The density of rain gauges
719 (in average, 1 every 180 km^2) and its time resolution (1 hour) limit the ability of the system
720 to monitor the variability of the rainfall field at smaller scales, thus reducing the skill of the
721 system to forecast flooding due to very local precipitation, especially in convective
722 situations. However, this factor did not seem to be critical for the case of January 2010
723 presented above: although intense rainfall was mainly localized in the southern part of the
724 catchment and gauges recorded maximum accumulations of 40 mm in 2 hours (see section
725 5.1), the system was able to diagnose the magnitude of the event and useful warnings were
726 issued. On the other hand, the number of stream gauges and their location (around 40 km
727 from the outlet of the basin) implies that the calibration of the rainfall-runoff model is
728 mostly valid for the upper part of the basin. Consequently, the simulations obtained
729 downstream (for instance in the area near Málaga, more urbanized than the upper part) are

730 based on an extrapolation of the calibrated parameters, which are assumed to be valid for
731 the entire basin. The lack of flow measurements downstream does not allow any
732 quantitative validation of the simulations.

733 (3) As it has been implemented here, the GFWS has been run with rainfall observations,
734 and, consequently, the results presented above assess the ability of the GFWS to emulate
735 the response of the catchment for two case studies. However, from the operational point of
736 view, it is also fundamental to analyse the ability of the system to forecast the hydrological
737 response of the basin (and resulting warnings) upon all the knowledge available up to the
738 present (see Todini 1988). By only using rainfall observations, the flow forecasting skill is
739 limited to the response time of the considered basin (Berenguer *et al*. 2005; Vivoni *et al*.
740 2006). On top of that, the time resolution of rainfall records (1 hour for rain gauge records)
741 and the data collection time (about 20 minutes) are factors that reduce the time between the
742 forecasts/warnings are issued and the inundations occur. That means the current
743 configuration of the GFWS (using only rain gauge data) may provide valuable flood
744 warnings only for basins larger than 200 km^2, with response times over 1 hour. In other
745 words, the system evaluates what is happening in the smallest basins and has some
746 predictive skill for the largest ones thanks to the response time of the basin.

747 In part, (2) can be addressed with the use of radar-based QPE maps (as illustrated for a
748 minor event in Section 5.3): these allow monitoring the space and time variability of the
749 rainfall field at resolutions fulfilling the requirements of rainfall-runoff model for small- to
750 medium-sized basins (see, among many others, Sempere-Torres *et al*. 1999; Rossa *et al*.
751 2005; Cole and Moore 2008; Corral *et al*. 2009; Delrieu *et al*. 2009). However, it has been
752 classically recognized that there are a number of errors (listed, e.g. by Zawadzki 1984;
753 Austin 1987; Joss and Waldvogel 1990) that affect radar-based QPE and that require the
754 implementation of sophisticated algorithms to mitigate their effect (also, the blending of
755 radar QPE maps with rain gauge measurements has shown significant improvements –see,
756 e.g. Velasco-Forero *et al*. 2009 ; Schiemann *et al*. 2010 and references therein-).

757 Radar rainfall products also allow generating very short-term rainfall forecasts (nowcasts)
758 that can be used to extend the time series of rainfall inputs to the rainfall-runoff model
759 [critical in point (3) above]. Previous works on this subject show significant improvements

760 in the quality of forecasted hydrographs (see Berenguer *et al*. 2005; Versini 2012; Vivoni *et*
761 *al*. 2006; Zappa *et al*. 2011): The anticipation of flow peaks could be extended for up to a
762 few hours in small to medium basins and, when included in the GFWS, should enable
763 improving the skill of the system for flood forecasting. Beyond these time horizons (critical
764 for flood management and rescue services to prepare and plan their actions), rainfall
765 forecasts based on the combination of radar-based products with numerical weather
766 prediction (NWP) precipitation outputs (as suggested by Li and Lai 2004; Lin *et al*. 2005;
767 Atencia *et al*. 2010) should be used. Also, other works (see Jasper *et al*. 2002; Zappa *et al*.
768 2010 and references therein) have shown the interest of coupling NWP precipitation
769 outputs for flood forecasting in small and medium catchments. In our case, it represents an
770 opportunity to fulfil the gap between the lead-times provided by EFAS (several days in
771 advance) and those provided by the GFWS (few hours in the best case). The 2 or 3 hours
772 gained by this combination are critical in crisis management. They should be useful to
773 anticipate the direct consequences of the current event and to optimize emergency services
774 resources. It should also allow to better anticipate small-scale event and to deliver warning
775 on smaller watersheds.

776 In this sense, it should be noted that the GFWS is ready to use any gridded rainfall product.
777 In particular, the GFWS is currently using the radar-based QPE and QPF products
778 generated with the EHIMI packages using observations from the Málaga radar (not
779 available for the analysed events). As discussed above, with the inclusion of these high-
780 resolution precipitation products we expect a better performance of the system, especially
781 for issuing warnings at local scales.

782 **Acknowledgments**

783 The authors would like to thank Red HIDROSUR (Southern Andalusia Hydrological
784 Network) and the AEMET (Spanish Meteorological Agency) for providing historical
785 hydrometeorological data on the Guadalhorce basin. We would also like to thank the Joint
786 Research Centre (JRC) for providing preliminary EFAS outputs for the studied cases. This
787 work has been carried out within the European 7th FP project IMPRINTS
788 (http://www.imprints-fp7.eu) and the Spanish projects FFGRad (CGL2009-13139) and
789 ProFEWS (CGL2010-15892), and has been supported by the environmental management

company EGMASA (currently, Agencia de Medio Ambiente y Agua de Andalucía, Consejería de Medio Ambiente - Junta de Andalucía). The second author is supported by a Ramón y Cajal grant of the Spanish Ministry of Science and Innovation (RYC2010-06521).

References

Alfieri, L., Velasco, D. and Thielen, J. (2011) Flash flood detection through a multi-stage probabilistic warning system for heavy precipitation events. Advances in Geosciences, 29: 69-75.

Atencia, A., Rigo, T., Sairouni, A., Moré, J., Bech, J., Vilaclara, E., Cunillera, J., Llasat, M.C. and Garrote, L. (2010) Improving QPF by blending techniques at the Meteorological Service of Catalonia. Natural Hazards and Earth System Sciences, 10(7): 1443-1455.

Austin, P.M. (1987) Relation between measured radar reflectivity and surface rainfall. Monthly Weather Review, 115: 1053-1070.

Barredo, J. I. (2007) Major flood disasters in Europe: 1950–2005. Natural Hazards, 42: 125–148.

Ben-Zvi, A. (2009) Rainfall intensity-duration-frequency relationships derived from large partial duration series. Journal of Hydrology, 367(1-2): 104-114.

Berenguer, M., Corral, C., Sánchez-Diezma, R. and Sempere-Torres, D. (2005) Hydrological Validation of a Radar-Based Nowcasting Technique. Journal of Hydrometeorology, 6(4): 532-549.

Berne, A., ten Heggeler, M., Uijlenhoet, R., Delobbe, L., Dierickx, P. and de Wit, M. (2005) A preliminary investigation of radar rainfall estimation in the Ardennes region and a first hydrological application for the Ourthe catchment. Natural Hazards and Earth System Sciences, 5: 267-274.

Blöschl, G. and Sivapalan, M. (1995) Scale issues in hydrological modelling: A review. Hydrological Processes, 9(3-4): 251-290.

Borga, M. (2008) Realtime guidance for flash flood risk management.

Borga, M., Boscolo, P., Zanon, F. and Sangati, M. (2007) Hydrometeorological analysis of the August 29, 2003 flash flood in the eastern Italian Alps. Journal of Hydrometeorology, 8(5): 1049-1067.

820 Borga, M., Degli Esposti, S. and Norbiato, D. (2006) Influence of errors in radar rainfall
821 estimates on hydrological modeling prediction uncertainty. Water Resources Research,
822 42(8): 1-14.

823 Carpenter, T.M. and Georgakakos, K.P. (2006) Intercomparison of lumped versus
824 distributed hydrologic model ensemble simulations on operational forecast scales. Journal
825 of Hydrology, 329(1-2): 174-185.

826 Cole, S.J. and Moore, R.J. (2008) Hydrological modelling using raingauge-and radar-based
827 estimators of areal rainfall. Journal of hydrology 358(3-4): 159-181.

828 Collier, C.G. (2007) Flash flood forecasting: what are the limits of predictability ?
829 Quarterly Journal of the Royal Meteorological Society, 133: 3-23.

830 Corral, C., Berenguer, M., Sempere-Torres, D. and Escaler, I. (2002) Evaluation of a
831 conceptual distributed rainfall-runoff model in the Besòs catchment in Catalunya using
832 radar information, Second European Conference on Radar Meteorology. European
833 Meteorological Society, Delft, Netherlands, pp. 409-415.

834 Corral, C., Sempere-Torres, D., Revilla, M. and Berenguer, M. (2000) A semi-distributed
835 hydrological model using rainfall estimates by radar. Application to Mediterranean basins.
836 Physics and Chemistry of the Earth, Part B: Hydrology, Oceans and Atmosphere, 25(10-
837 12): 1133-1136.

838 Corral, C., Velasco, D., Forcadell, D., Sempere-Torres, D. and Velasco, E. (2009)
839 Advances in radar-based flood warning systems. The EHIMI system and the experience in
840 the Besos flash-flood pilot basin. In: P. Samuels, S. Huntington, W. Allsop and J. Harrop
841 (Editors), Flood Risk Management: Research and Practice. Taylor & Francis Group,
842 London.

843 Costa, J.E. and Jarett, R.D. (2008) An evaluation of selected extraordinary floods in the
844 United States reported by the US, Geological Survey and implications for future
845 advancement of flood science, Reston, Virginia.

846 Creutin, J.-D. and Borga, M. (2003) Radar hydrology modifies the monitoring of flash
847 flood hazard. Hydrological Processes, 17(7): 1453-1456.

848 Creutin, J.D., Borga, M., Lutoff, C., Scolobig, A., Ruin, I. and Créton-Cazanave, L. (2009)
849 Catchment dynamics and social response during flash floods: the potential of radar rainfall
850 monitoring for warning procedures. Meteorological Applications, 16(1): 115-125.

851 Delrieu, G., Braud, I., Berne, A., Borga, M., Boudevillain, B., Fabry, F., Freer, J., Gaume,
852 E., Nakakita, E., Seed, A., Tabary, P. and Uijlenhoet, R. (2009) Weather radar and
853 hydrology. Advances in Water Resources, 32(7): 969-974.

854 Delrieu, G., Creutin, J.D. and Andrieu, H. (1995) Simulation of Radar Mountain Returns
855 Using a Digitized Terrain Model. Journal of Atmospheric and Oceanic Technology, 12(5):
856 1038-1049.

857 Fabry, F. and Zawadzki, I. (1995) Long-Term Radar Observations of the Melting Layer of
858 Precipitation and Their Interpretation. Journal of the Atmospheric Sciences, 52(7): 838-
859 851.

860 Francés, F. and Benito, J. (1995) La modelización ditribuida con pocos parametros de las
861 crecidas. Ingenieria del Agua, 2(4): 7-24.

862 Franco, M. (2008) Estimación cuantitativa de la lluvia mediante radar meteorológico.
863 Corrección del error asociado a la variación vertical de la reflectividad, Universitat
864 Politècnica de Catalunya, Barcelona, Spain, 251 pp.

865 Franco, M., Sanchez-Diezma, R. and Sempere-Torres, D. (2006) Improvements in weather
866 radar rain rate estimates using a method for identifying the vertical profile of reflectivity
867 from volume radar scans. Meteorologische Zeitschrift, 15(5): 521-536.

868 Gaume, E., Bain, V., Bernardara, P., Newinger, O., Barbuc, M., Bateman, A.,
869 Blaskovicov·, L., Blöschl, G., Borga, M., Dumitrescu, A., Daliakopoulos, I., Garcia, J.,
870 Irimescu, A., Kohnova, S., Koutroulis, A., Marchi, L., Matreata, S., Medina, V., Preciso,
871 E., Sempere-Torres, D., Stancalie, G., Szolgay, J., Tsanis, I., Velasco, D. and Viglione, A.

(2009) A compilation of data on European flash floods. Journal of Hydrology, 367(1-2): 70-78.

Georgakakos, K.P. (2006) Analytical results for operational flash flood guidance. Journal of Hydrology, 317(1-2): 81-103.

Germann, U., Berenguer, M., Sempere-Torres, D. and Zappa, M. (2009) REAL - Ensemble radar precipitation estimation for hydrology in a mountainous region. Quarterly Journal of the Royal Meteorological Society, 135(639): 445-456.

Hajat, S; Ebi, KL; Kovats, S; Menne, B; Edwards, S; Haines, A; (2003) The human health consequences of flooding in Europe and the implications for public health: a review of the evidence. Applied Environmental Science and Public Health, 1: 13-21.

IACOW (1982) Guidelines for determining flood flow frequency. Bulletin 17B of the Hydrology Subcommittee. US Geological Survey, Reston, VA.

Jasper, K., Gurtz, J. and Lang, H. (2002) Advanced flood forecasting in Alpine watersheds by coupling meteorological observations and forecasts with a distributed hydrological model. Journal of Hydrology, 267(1-2): 40-52.

Javelle, P., Fouchier, C., Arnaud, P. and Lavabre, J. (2010) Flash flood warning at ungauged locations using radar rainfall and antecedent soil moisture estimations. Journal of Hydrology, 394(1-2): 267-274.

Joss, J. and Waldvogel, A. (1990) Precipitation measurement and hydrology. In: D. Atlas (Editor), Radar in Meteorology. Ed., American Meteorological Society, Boston (USA), pp. 577-606.

Lavabre, J. and Gregoris, Y. (2006) AIGA: un dispositif d'alerte des crues. Application à la région méditerranéenne française, Fifth FRIEND World Conference. IAHS, Havana, Cuba, pp. 214-219.

Li, P.W. and Lai, E.S.T. (2004) Short-range quantitative precipitation forecasting in Hong Kong. Journal of Hydrology, 288(1-2): 189-209.

898 Lin, C., Vasi, S., Kilambi, A., Turner, B. and Zawadzki, I. (2005) Precipitation forecast
899 skill of numerical weather prediction models and radar nowcasts. Geophys. Research
900 Letters, 32(14): L14801.

901 Liu, Y. , Weerts, A. H. , Clark, M. , Hendricks Franssen, H.-J. , Kumar, S., Moradkhani, H.,
902 Seo, D.-J. , Schwanenberg, D., Smith, P., van Dijk, A. I. J. M. , van Velzen, N., He, M.,
903 Lee, H., Noh, S. J. , Rakovec, O. and Restrepo, P. (2012) Advancing data assimilation in
904 operational hydrologic forecasting: progresses, challenges, and emerging opportunities.
905 Hydrology and Earth System Sciences, 16: 3863-3887

906 Meon, G. (2006) Past and present challenges in flash flood forecasting, First International
907 Workshop on Flash Flood Forecasting, San Jose, Costa Rica, pp. 2.

908 Merz, R. and Blöschl, G. (2009) A regional analysis of event runoff coefficients with
909 respect to climate and catchment characteristics in Austria. Water Resources Research,
910 45(1): W01405.

911 Michel, C., AndrÈassian, V. and Perrin, C. (2005) Soil Conservation Service Curve
912 Number method: How to mend a wrong soil moisture accounting procedure? Water Resour.
913 Res., 41(2): W02011.

914 Mockus, V. (1957) Use of storm and watersheds characteristics in synthetic hydrograph
915 analysis and application. Soil Conservation Service. U.S. Dept. of Agriculture, Washington
916 (USA).

917 MOPU (1990) Norma 5.2-IC, drenaje superficial: instrucción de carreteras. Ministerio de
918 Obras Públicas y Urbanismo, Dirección General de Carreteras, Madrid.

919 MOPU (1999) Máximas Lluvias de la España peninsular. Ministerio de Obras Públicas y
920 Urbanismo, Dirección General de Carreteras, Madrid.

921 Moulin, L., Gaume, E. and Obled, C. (2009) Uncertainties on mean areal precipitation:
922 assessment and impact on streamflow simulations. Hydrology and Earth System Sciences,
923 13(2): 99-114.

924 Nash, J.E. and Sutcliffe, J.V. (1970) River flow forecasting through conceptual models part
925 I — A discussion of principles. Journal of Hydrology, 10(3): 282–290.

926 Norbiato, D., Borga, M., Degli Esposti, S., Gaume, E. and Anquetin, S. (2008) Flash flood
927 warning based on rainfall thresholds and soil moisture conditions: An assessment for
928 gauged and ungauged basins. Journal of Hydrology, 362(3-4): 274-290.

929 Norbiato, D., Borga, M., Sangati, M. and Zanon, F. (2007) Regional frequency analysis of
930 extreme precipitation in the eastern Italian Alps and the August 29, 2003 flash flood.
931 Journal of Hydrology, 345: 149-166.

932 Perrin, C., Michel, C., Andréassian, V. Does a large number of parameters enhance model
933 performance? Comparative assessment of common catchment model structures on 429
934 catchments. Journal of Hydrology, 242(3-4): 275-301.

935 Reed, S., Koren, V., Smith, M., Zhang, Z., Moreda, F., Seo, D.-J. and Participants, D.
936 (2004) Overall distributed model intercomparison project results. Journal of Hydrology,
937 298(1-4): 27-60.

938 Reed, S., Schaake, J. and Zhang, Z. (2007) A distributed hydrologic model and threshold
939 frequency-based method for flash flood forecasting at ungauged locations. Journal of
940 Hydrology, 337(3-4): 402-420.

941 Rossa, A., Bruen, M., Fruehwald, D., Macpherson, B., Holleman, I., Michelson, D. and
942 Michaelides, S. (2005) Use of Radar Observations in Hydrology and NWP models,
943 Brussels. 292 pp.,

944 Rozalis, S., Morin, E., Yair, Y. and Price, C. (2010) Flash flood prediction using an
945 uncalibrated hydrological model and radar rainfall data in a Mediterranean watershed under
946 changing hydrological conditions. Journal of Hydrology, 394(1-2): 245-255.

947 Sánchez-Diezma, R., Sempere-Torres, D., Delrieu, G. and Zawadzki, I. (2001) An
948 improved methodology for ground clutter substitution based on a pre-classification of

precipitation types, 30th Int. Conf. on Radar Meteorology. Amer. Meteor Soc., Munich, Germany, pp. 271-273.

Schiemann, R., Liniger, M.A. and Frei, C. (2010) Reduced space optimal interpolation of daily rain gauge precipitation in Switzerland. J. Geophys. Res., 115(D14): D14109.

Sempere-Torres, D., Corral, C., Raso, J. and Malgrat, P. (1999) Use of weather radar for combined sewer overflows monitoring and control. Journal of Environmental Engineering, 125: 372-380.

Siccardi, F., Boni, G., Ferraris, L. and Rudari, R. (2005) A hydrometeorological approach for probabilistic flood forecast. Journal of Geophysical Research, 110: D05101.

Szymkiewicz, R. (2002) An alternative IUH for the hydrological lumped models. Journal of Hydrology, 259(1-4): 246-253.

Tanguy, J.-M., Carriere, J.-M., le Trionnaire, Y. and Schoen, R. (2005) Réorganisation de l'annonce des crues en France. La Houille Blanche, 2: 44-48.

Thielen, J., Bartholmes, J., Ramos, M.-H. and de Roo, A. (2009) The European Flood Alert System - Part 1: Concept and development. Hydrology and Earth System Sciences, 13(2): 125-140.

Todini, E. (1988) Rainfall-runoff modeling - Past, present and future. Journal of Hydrology, 100(1-3): 341-352.

Van Der Knijff, J.M., Younis, J. and De Roo, A.P.J. (2010) LISFLOOD: a GIS-based distributed model for river basin scale water balance and flood simulation. International Journal of Geographical Information Science, 24(2): 189-212.

Velasco-Forero, C.A., Sempere-Torres, D., Cassiraga , E.F. and Gómez-Hernández, J.J. (2009) A non-parametric automatic blending methodology to estimate rainfall fields from rain gauge and radar data. Advances in Water Resources, 32: 986-1002.

973 Versini, P.-A. (2012) Use of radar rainfall estimates and forecasts to prevent flash flood in
974 real time by using a road inundation warning system. Journal of Hydrology, 416-417: 157-
975 170.

976 Versini, P.-A., Gaume, E. and Andrieu, H. (2010) Application of a distributed hydrological
977 model to the design of a road inundation warning system for flash flood prone areas.
978 Natural Hazards Earth System Sciences, 10(4): 805-817.

979 Versini, P.-A., Velasco, M., Cabello, A., Sempere-Torres D. (2013). Hydrological impact
980 of forest fires and climate change in a Mediterranean basin. Natural Hazards 66(20): 609-
981 628.

982

983 Viviroli, D., Zappa, M., Gurtz, J. and Weingartner, R. (2009) An introduction to the
984 hydrological modelling system PREVAH and its pre- and post-processing-tools.
985 Environmental Modelling and Software, 24(10): 1209-1222.

986 Vivoni, E.R., Entekhabi, D., Bras, R.L., Ivanov, V.Y., Van Horne, M.P., Grassotti, C. and
987 Hoffman, R.N. (2006) Extending the Predictability of Hydrometeorological Flood Events
988 Using Radar Rainfall Nowcasting. Journal of Hydrometeorology, 7(4): 660-677.

989 Weeks, W.D. and Boughton, W.C. (1987) Tests of ARMA model forms for rainfall-runoff
990 modelling. Journal of Hydrology, 91(1-2): 29-47.

991 Wright, D.B., Smith, J.A., Villarini, G., Baeck, M.L. (2013) Estimating the frequency of
992 extreme rainfall using weather radar and stochastic storm transposition. Journal of
993 Hydrology. Article in Press.

994 Zappa, M., Beven, K.J., Bruen, M., Cofiño, A.S., Kok, K., Martin, E., Nurmi, P., Orfila, B.,
995 Roulin, E., Schröter, K., Seed, A., Szturc, J., Vehviläinen, B., Germann, U. and Rossa, A.
996 (2010) Propagation of uncertainty from observing systems and NWP into hydrological
997 models: COST-731 Working Group 2. Atmospheric Science Letters, 11(2): 83-91.

998 Zappa, M., Jaun, S., Germann, U., Walser, A. and Fundel, F. (2011) Superposition of three
999 sources of uncertainties in operational flood forecasting chains. Atmospheric Research,
1000 100(2-3): 246-262.

1001 Zawadzki, I. (1984) Factors affecting the precision of radar measurements of rain
1002 Conference on Radar Meteorology, 22nd. American Meteorological Society, Zurich,
1003 Switzerland, pp. 251-256.

1004

1005

1006

1007 **Figure captions**

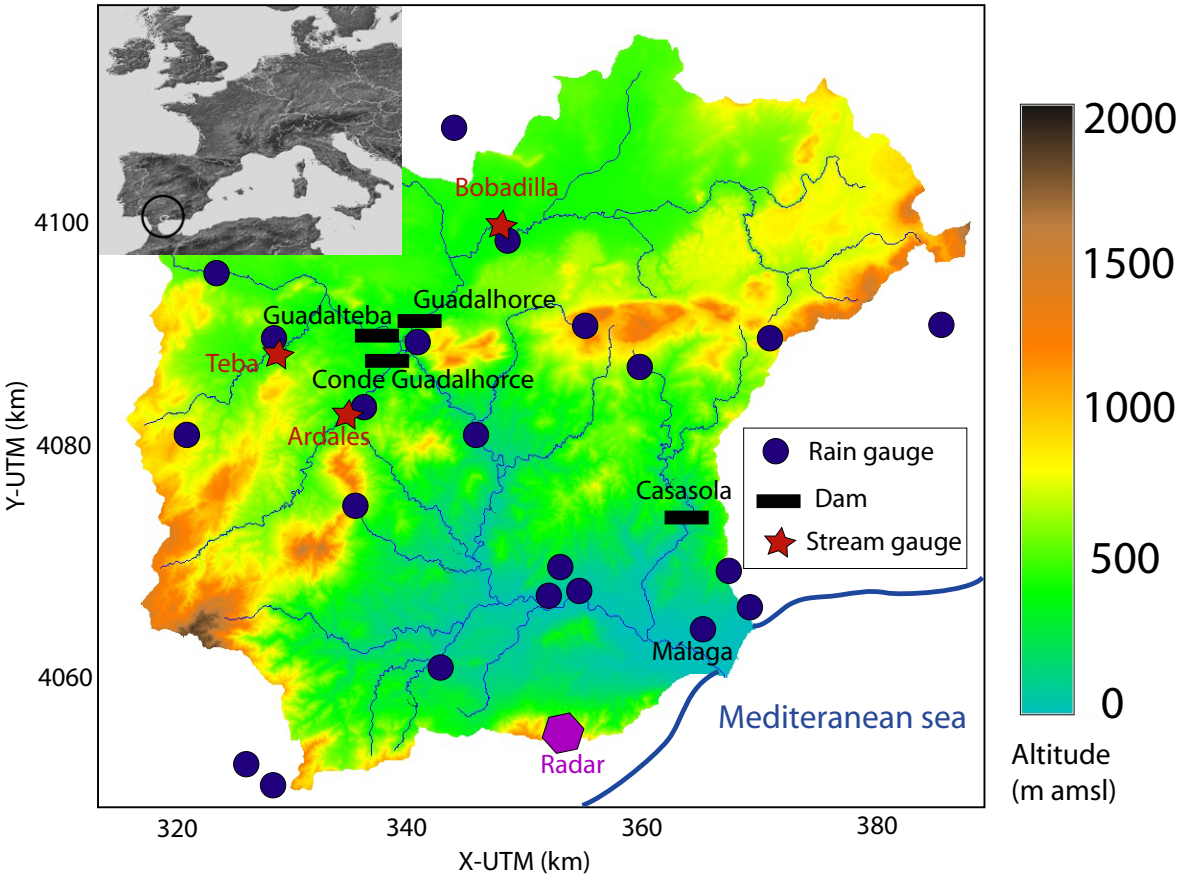

1008

1009 Figure 1. The Guadalhorce basin and its hydro-meteorological sensors

1010

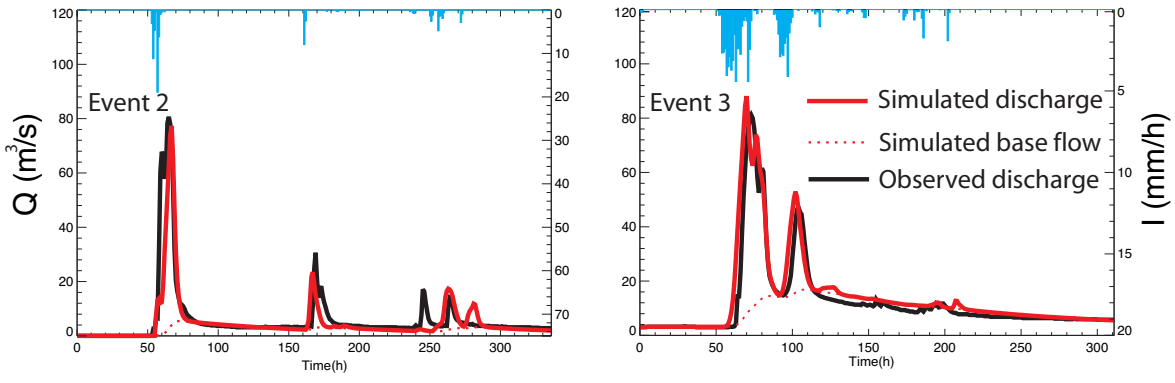

1011

1012 Figure 2. Comparison between observed (black line) and simulated (red line) discharges on
1013 Bobadilla basin. The left vertical axis represents the discharge (in m3/s). The right vertical
1014 axis represents the rainfall intensity (in mm/h).

1015

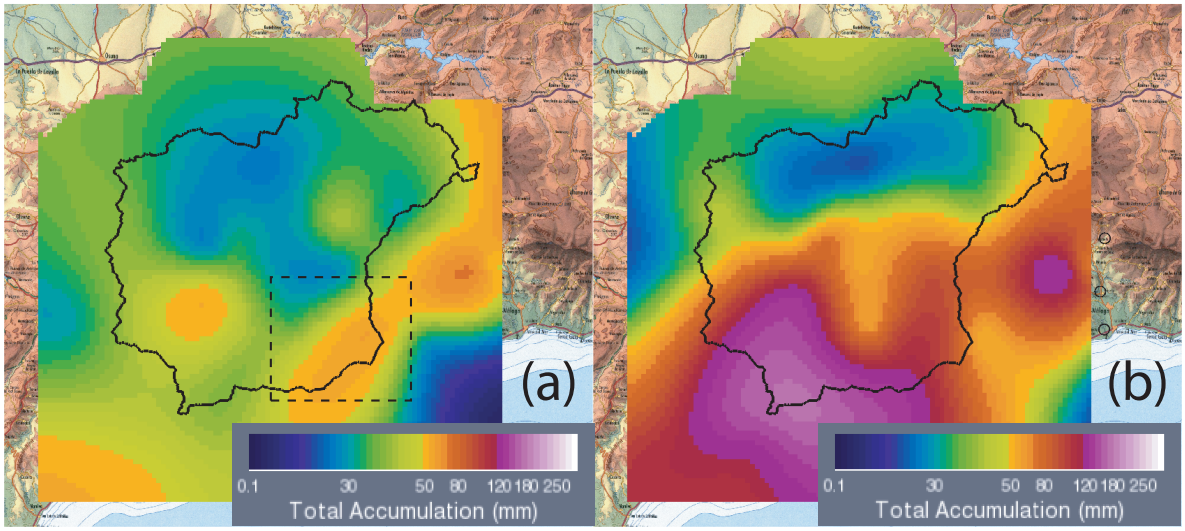

Figure 3. Total estimated precipitation accumulation estimated from rain gauges for (a) 6-7 January 2010, and (b) 15-16 February 2010.

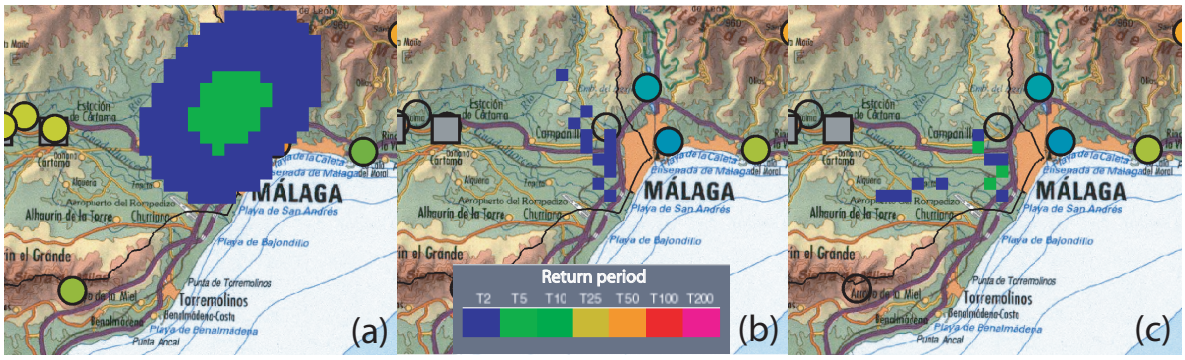

Figure 4. Flood warnings issued on 7 January 2010 based on: (a) point rainfall at 9:00 UTC, (b) aggregated rainfall at 10:00 UTC, and (c) simulated discharges at 10:00 UTC. This area around Málaga is the one defined by the dotted square in Fig. 3. The circles indicate the presence of the rain gauges. The solid red ellipses correspond to the effective flooding

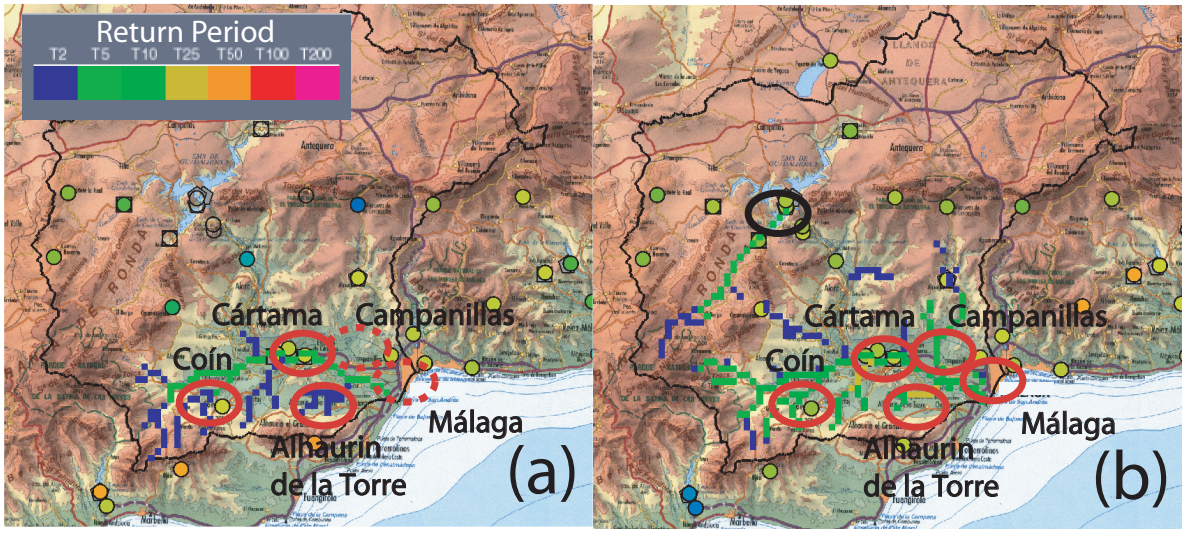

Figure 5. Flood warnings issued on 16 February 2010 based on: (a) Aggregated rainfall at 6:00, and (b) and simulated discharge at 7:00. Flooded locations are surrounded in red. The solid red ellipses correspond to the forecasted flooding and the dotted ellipses to the missed flooding. The black ellipse corresponds to the false alarm at Conde Guadalhorce dam.

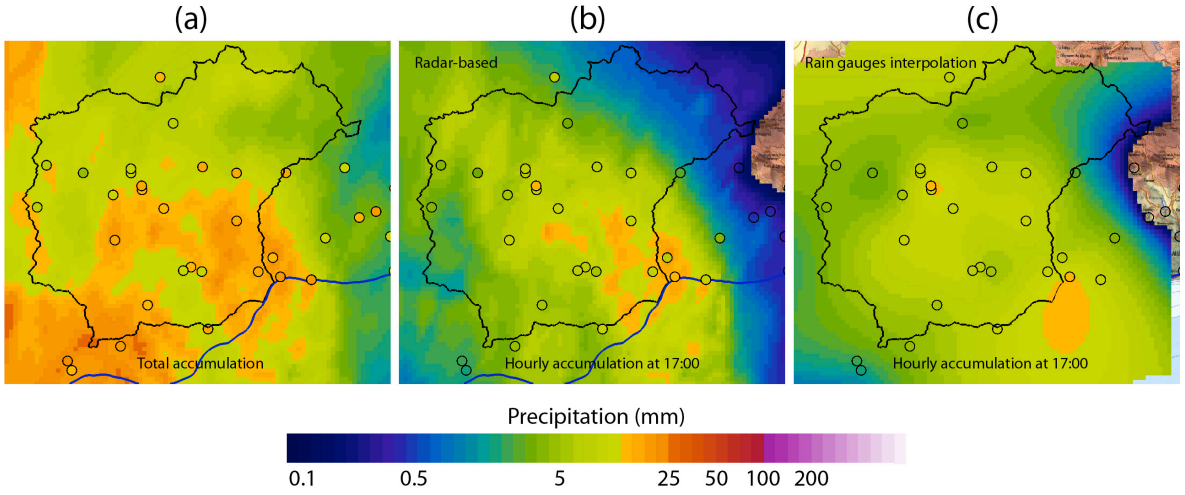

Figure 6. Results obtained for the 21 April 2011 event: (a) total precipitation accumulated from radar-based estimates, (b) hourly rainfall field at 17:00 UTC computed by using radar-based estimates, (c) hourly rainfall field at 17:00 UTC interpolated from rain gauges. The circles represent the rain gauges and their observed values.

Table captions

Table 1

	Event 1	Event 2	Event 3	Event 4	Event 5	Event 6	Event 7	Event 8
Qmax [m^3/s]	44.4	80.7	81.2	27.2	20.8	42.6	22.7	84.3
Rainfall [mm]	59.6	78.6	82.3	57.1	34.4	23.3	24.5	97.5
NE	-0.49	0.70	0.84	-1.80	-0.24	0.76	0.57	0.06

Table 1. Characteristics of the events selected for the calibration of the rainfall-runoff model in the Bobadilla watershed. In the table, Qmax is the maximum measured peak flow, Rainfall the total amount of precipitation on the sub-catchment, and NE the Nash efficiency characterizing the calibration assessment.

Table 2

	Bobadilla		Teba		Ardales	
Event	Qmax [m^3s^{-1}]	NE	Qmax [m^3s^{-1}]	NE	Qmax [m^3s^{-1}]	NE
6-7 January 2010	100	0.69	60	0.53	-	-
15-16 February 2010	80	0.62	65	0.57	33	0.35

Table 2. Characteristics of test case studies and results obtained with the rainfall-runoff model at the gauged watersheds. In the table, Qmax is the maximum measured peak flow, and NE the Nash efficiency characterizing the calibration assessment. Note that, as explained in Section 3.3, Teba and Ardales gauges were not used in the calibration of the rainfall-runoff model.